A Comprehensive Kinetic Modelling Study of CO_2 Gasification of Char Derived from Food Waste

Ainul N. Izaharuddin[1], Manosh C. Paul[1]*, Kunio Yoshikawa[2], Sarut Theppitak[2], Xin Dai[2]

[1]Systems, Power & Energy Research Division, James Watt School of Engineering, University of Glasgow, Glasgow G12 8QQ, United Kingdom

[2] School of Environmental and Society, Tokyo Institute Technology, Yokohama 226-8502, Japan

*Corresponding author: Manosh.Paul@glasgow.ac.uk; Tel: +44(0)141 330 8466

Abstract

Chemical kinetics for char originated through biomass devolatization are the essential requirements for studying the thermochemical processes of gasification. While the char kinetics for typical biomass and coal feedstocks are numerously available in the literature, the gasification kinetics of char produced from food waste (FW) in CO_2 environment are still unknown. Further, the chemical compositions of char and FW are significantly different than those from woody biomass and coal. To address this, an in-depth kinetic study for the CO_2 gasification of FW char is conducted in this paper. FW is initially pyrolysed at 800°C, and char sample is sieved in the range 53-100μm before being gasified in a thermogravimetric analyser (TGA) under CO_2 atmosphere at temperatures of 850°C, 900°C and 950°C. The experimental results show that the char conversion rate increases with the reaction times and temperature. Using the TGA data, three different kinetic models namely volumetric model (VM), shrinking core model (SCM) and random pore model (RPM), are developed and their effectiveness is thoroughly investigated. Comparing with the experimental results, SCM shows having a high regression at 850°C, while RPM at 900°C and 950°C. A power law (PL) model is also introduced and it demonstrates that its regression is higher than 99% at every gasification temperature investigated. Therefore, PL most precisely predicts the gasification kinetics, which also agrees well with RPM.

Keywords: Food waste char, CO_2 gasification, kinetic study, power law model

Introduction

A great amount of food waste produced around the world causes the environmental problem by producing methane in landfill. According to the recent report by the UK's Department for Environment, Food and Rural Affairs (DEFRA), approximately 10 million tonnes of food and drink are wasted in the food chain annually, mostly produced in the households, manufacturing, and pre-farm gate, which is equal to approximately one quarter of the food purchased in the United Kingdom [1].

Lin et al. [2] reported the current situation and global perspective of food waste as a valuable resource for the chemical, materials and fuel production. The food waste supply chain (FWSC) is also recognised it as a renewable feedstock to enhance the development of innovative and sustainable strategies for the reuse of food waste. Pfaltzgraff et al. [3] illustrated the high value of chemicals available in food waste biomass and also showed the volume of FWSC available globally. This, therefore, shows that food waste has the great potential to produce energy suitable for human needs. Further, food waste contains heterogeneous compositions consisting of carbohydrates (sugar, starch, and cellulose), lipids, protein, lignin and ash [2, 4]. The composition of food waste, according to the type of food waste, consists of rice and vegetables (carbohydrates), also meat and eggs containing proteins and lipids [5]. With these mixtures of FW, carbon content in the FW sample could generally be higher than a typical biomass. Note that the most biomass has less than 60% C, e.g. beech wood, pine sawdust, apricot pulp, empty palm fruit bunches, coconut shell and wood. However, FW has lower oxygen content than that of those biomass [6] and thus different types of FW contain different chemical compositions, giving the different ultimate analysis.

With regard to the FW to energy, Ahmed and Gupta [7], Ko et al. [8], and Tanaka et al. [9] examined the FW char gasification by using steam as an agent, while Okajima et al. [10] used high pressure superheated steam. Ahmed and Gupta [7] reported that the FW gasification produced more syngas, hydrogen and energy compared with pyrolysis. Ko et al. [8] performed an experimental work on food waste gasification by using a fluidized bed with steam, which is a thermal method of treating food waste to be carbonized as a solid fuel and to produce synthesis gas. Tanaka et al. [9] identified the basic characteristics of food waste and food ash in the steam gasification to design a gasifier. This study reported the effects of this highly efficient system in producing hydrogen by adding alkali components to food ash, while calcium oxide in an ash absorbed CO_2 generated in the steam gasification. Montesinos

et al. [11] analysed the grapefruit skin char gasification in CO_2 and steam, and showed the activation energy in CO_2 gasification is higher than steam gasification. Several researchers used fruit waste and agro-food as a feedstock for gasification, such as rice husk in CO_2 gasification [12]; almond shells in steam gasification [13]; and aloe vera rind, banana peel, coconut shell, lemon peel, orange peel, pineapple peel and sugarcane bagasse in supercritical water gasification [14]. Moreover, a simulation of FW gasification by using Aspen Plus in steam injection was performed by Ramzan et al. [15]. Hla et al. [16] presented the chars reactivity from municipal solid waste (MSW) in CO_2 gasification, which included the food waste sample to produce around 252 kJ/mol activation energy. Therefore, based on the previous research reported, gasification of FW seems to be a potential method to convert FW to energy.

Furthermore, kinetic mechanism of CO_2 gasification was widely investigated by a number of researchers. For example, Tancredi et al. [17] gasified the eucalyptus wood char with CO_2 in both isothermal and non-isothermal conditions, which produced 230-261 $kJmol^{-1}$ of activation energies at a temperature of 700°C. Tran et al. [18] also explored the isothermal and non-isothermal procedures at a temperature of 1123K and 400-1273K respectively, in the kinetic studies of CO_2 gasification. For the isothermal CO_2 gasification, three models were tested namely random pore model (RPM), shrinking core model (SCM) and homogeneous model (HM). Through that research, it was reported that the HM was not applicable to represent the isothermal gasification, while the RPM was found to be the most applicable model. The RPM of woodchips was also examined by Ahmed and Gupta [19], while Lopez et al. [20] developed several modified RPMs, and Yuan et al. [21] used RPM in the kinetic study of char CO_2 gasification at temperature 850°C – 1050°C. Bhat et al. [12] studied the kinetics of rice husk gasification by using two kinetic models; HM and SCM at 750°C, 800°C, 850°C, and 900°C. Tangsathitkulchai et al. [22] made a comparison of the kinetic models in CO_2 gasification of coconut-shell chars at 250-750°C by using VM, SCM, RPM and modified volume-reaction model (MVRM). Rollinson and Karmakar [23] examined the reactivity of biomass in CO_2 gasification for fixed-bed gasification by using RPM. Whereas Gomez and Mahinpey [24] presented a new method to reduce interparticle diffusion of coal in steam and CO_2 gasification at temperature 800°C, 850°C, and 900°C. Based on the previous studies, most of the research used the volumetric model (VM) or HM, SCM and RPM. Parvez et al. [25], however, demonstrated the catalytic effect on the CO_2 gasification of coal. Prabowo et al. [26] also developed the CO_2-recycling gasification system to implement

the carbon-negative power system . It is important to discover the reaction rate properties through the kinetic study of char gasification, allowing investigation of the gasification process in a gasifier.

The thermochemical reactions taking place in every zone of a gasifier are controlled by the kinetic parameters as demonstrated in several recent studies, e.g. see [27-29]. Char produced from the biomass devolatization is gasified through the reduction zone in a downdraft gasifier, which is a rate limiting step for the whole process and much slower than the other reactions in devolatilization and oxidation [18]. Enhancing the reactivity of char, particularly that occurs with the Boudouard reaction in which char is reacted with CO_2 to produce CO, would therefore have significant benefit in biomass gasification. However, a wide range of variation in the kinetic parameters for the Boudouard reaction available in the published literatures ([30-37]) makes the task of selecting the suitable kinetics for the gasification of char derived from the food waste extremely difficult. In fact, no study, to the best of the authors' knowledge, to-date is conducted on the FW char gasification whereas the kinetic parameters for coal char gasification are numerous, as per the above reference papers. Further, coal char gasification significantly increases the reaction activation energy due to its higher C content (~68%–76%) but with low O content 7-12% [36]. This is, therefore, brought in another interesting point and research question that addresses the development of char kinetics in CO_2 gasification for FW as its compositions are different from coal and other biomass.

In this research, thermogravimetric analysis (TGA) is performed to examine the gasification kinetics of FW char, with the aim to establish a kinetic theory supporting the FW char gasification in CO_2 environment. With regard to the gasification rate, Blasi [38] suggested that the gasification rate is affected by the several factors such as heat, gasification temperature, temperature in pyrolysis stage, feedstock, and composition of inorganic matter. Furthermore, the reactivity of char is affected by the several other parameters including the thermal history of char, the char pore structure and the char chemical composition (Molina and Mondragon [39]). Therefore, the kinetic study, presented in this work, includes an in-depth investigation of the processes of the char conversion, the gasification rates and the char reactivity. The study is performed at varying temperatures of 850°C, 900°C and 950°C, with an ultimate goal to accomplish a kinetic rate equation for the CO_2 gasification of FW char.

The study first introduces the conventional kinetic methods, already presented in the literature (such as VM, SCM and RPM), and their applicability in the context of this research is investigated with a detailed regression analysis. This is then followed by the development and application of a new power law (PL) kinetic model to determine the best fitted kinetic parameter data of the activation energy E_a and the pre-exponential factor A for the FW char CO_2 gasification. This PL model can be used for certain char samples to produce the most fitted kinetic parameters if the sample fails to fit with the conventional kinetic methods. The results obtained from the different kinetics models are also compared against each other and the suitability of the new PL kinetic model is demonstrated.

The experimental procedure

The experiment of FW char gasification started with food waste collection, followed by pyrolysis and isothermal CO_2 gasification in a thermogravimetric analyser. The food waste consisted of 60% fried chicken, 20% spinach, 5% green onion, 10% corn and 5% sauces. To produce a homogenous sample, the food waste after collection was mixed up and the sample was then dried for a day at a temperature of 105°C, in the laboratory oven. The dry sample was pyrolyzed at a temperature of 800°C in a reactor, and char produced was sieved at range 53 - 100μm before being gasified in thermogravimetric analyser.

Ultimate and proximate analyses of the FW char were also conducted to investigate its chemical contents, and these results are presented in Table 1. The samples were analysed at the Suzukakedai Materials Analysis Division, Technical Department, Tokyo Institute of Technology, for their ultimate and proximate analyses. As seen, carbon content in the FW char is found to be higher than that of a typical biomass such as woodchip which contains ~52% C [19]. Most of the other types of biomass e.g. beech wood, pine sawdust, apricot pulp, empty palm fruit bunches, coconut shell and wood also contains less than 60% C, but with higher O than that of the FW char [6, 19]. Among the other studies on the chemical compositions of FW reported in the literature, Jayasena et al. [40] particularly showed that the chemical contents in cooked chicken are hydrocarbons, aldehydes, ketones, esters and carboxylic acid [41]. While, Tang et al. [42] reported that fried and heated chicken contains several thiazoles including C_4 to C_8 n-alkyl and alkylthiazoles with longer 2 alkyl substituents (C_{13} to C_{15}), which give the main essence of high carbon contents in fried chicken. Furthermore, spinach, green onion and corn in the FW are the category of vegetables containing carbohydrates, proteins, lipids, organic acids, and high content of minerals and

vitamins [43]. Therefore, with these mixtures of FW and also since carbohydrate consists of cellulose $(C_6H_{10}O_5)_n$, it gave high carbon content in the sample.

Table 1 Ultimate and proximate analysis results of FW char

Ultimate Analysis (%)		**Proximate Analysis (%)**	
Carbon	60.07	**MC**	0.96
Hydrogen	8.57	**VM**	83.44
Oxygen	31.37	**FC**	14.01
		Ash	1.59

TGA of CO_2 gasification

Isothermal CO_2 gasification of food waste experiment was carried out by using a thermogravimetric analyser (Shimadzu DTG-60H with thermal analyser TA-60WS). A schematic diagram of the thermogravimetric analyser (TGA) was already shown in the previous research by Kim et al. [44]*Experimental conditions*

- Samples: 5.46 mg, 8.07 mg and 8.15 mg of FW char
- Gasification temperatures: 850°C, 900°C and 950°C
- Atmosphere: CO_2
- Gas flow rate: 150 ml/min

Initially, the sample was loaded into the thermogravimetric pan and then it was heated to 100°C with a heating rate of 50°C/min and held for 5minutes in N_2 atmosphere. The temperature was then increased to 850°C, 900°C and 950°C, respectively, with a 50°C/min heating rate in the CO_2 atmosphere to start the CO_2 gasification process. Further, as already reported in the most recent study by Hungwe et al. [45], that the chosen flow rate of 150 ml/min was high enough for the reduction of gas equilibration time when switching from N_2 to CO_2. The gas flow rate was adequate to maintain a constant reaction atmosphere in the TGA during the CO_2 gasification and also eliminated any external diffusion effects associated with the particle size distribution and samples [45].

Figure 1 shows the temperature profiles of FW char at different temperatures of the isothermal CO_2 gasification. As mentioned, the temperature increase rate was constantly 50°C/min for every temperature. Then the FW char was held for 60 minutes at the temperature of 850°C, 41 minutes at 900°C and 18 minutes at 950°C. At the beginning of the process, the temperature was increased gradually, and at 1.3 minutes, the temperature fluctuated a little before it was steadily increased until it reached the temperature required. The fluctuation was because of the hold time to ensure that all moisture evolved [23].

Figure 2 also shows that the devolatilization (pyrolysis) occurred at a low temperature before it reached the gasification temperature, detailed in the next figure.

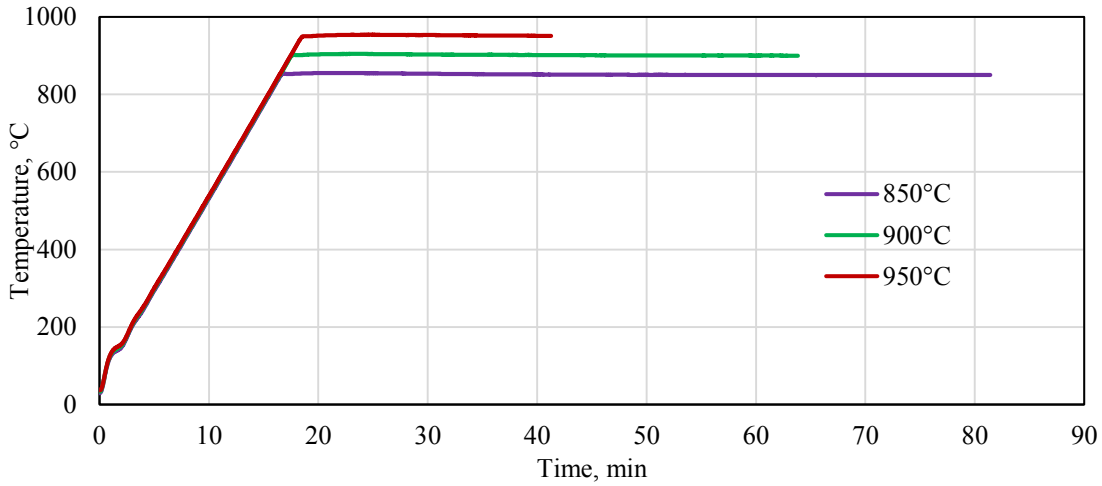

Figure 1 TGA temperature profiles at 850°C, 900°C, and 950°C

Figure 2 shows the thermogravimetric-differential thermogravimetry (TGA-DTG) profiles of the FW char at different temperatures, which was designed to examine the kinetic study of gasification in the CO_2 environment. As shown in the figure, the process started with devolatilization (pyrolysis), and was followed by CO_2 gasification for a certain time depending on the temperature selected. In the first 5 minutes, N_2 was injected into the system, since N_2 accommodated a less reactive atmosphere for the TGA. Then, the system automatically changed to CO_2 environment to proceed for CO_2 gasification.

As also shown in the DTG graphs in Figure 2, the first negative peak at an early stage (marked by the circle) shows the water removal from char where the most volatile substances are released at an early stage of the process (Trivedi et al. [46]). H and O contents of the char are also released and amorphous material is removed at the devolatilization zone [38].

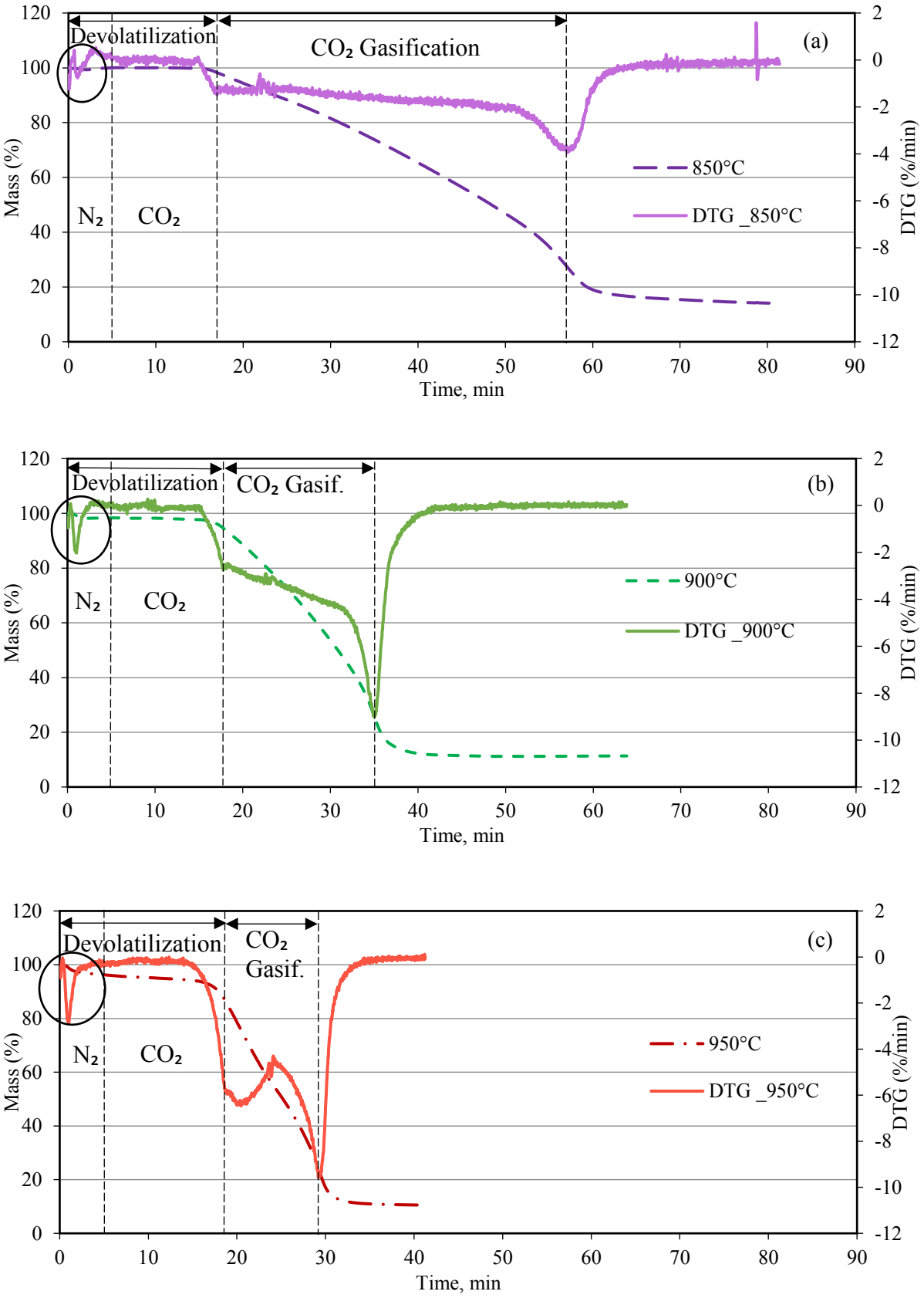

Figure 2 Thermogravimetric and DTG profiles at temperature (a) 850°C, (b) 900°C and (c) 950°C

After five minutes, CO_2 is injected to create the CO_2 environment in the system, which is still in the devolatilization zone and the char is decreased slowly until it is sustained over a certain time. The CO_2 gasification is started at the first negative peak point during the mass loss until the final peak of the gasification process is reached. This part therefore shows the process of gasification with the precise time interval.

Furthermore, at the temperature of 850°C, the devolatilization lasted for 11 minutes before the CO_2 gasification which took about 40 minutes to produce the final solid yield (ash) of approximately 14% of 5.46mg FW char. While at the temperature of 900°C, the devolatilization lasted for 17.8 minutes, then it was followed by CO_2 gasification for 35 minutes to produce 11.3% of ash. Finally, at 950°C, it took 20.4 minutes before CO_2 gasification took place, after which it took 11 minutes of CO_2 gasification to produce 10.5% of ash. It is further shown that the char at high temperature took more time for the devolatilization process but shorter for the CO_2 gasification. Therefore, the char is gasified rapidly at a high temperature, as gasification at a high temperature enhanced the endothermic Boudouard reaction, $C + CO_2 \rightarrow 2CO$ [20]. The finding is also supported by the temperature graph (see Figure 1) since the gasification temperature is one of the factors that affected the reactivity of the chars [38].

Kinetic modelling

Isothermal gasification kinetic model was initially developed based on the volumetric model (VM), the shrinking core model (SCM) and the random pore model (RPM) (Tancredi et al [17], Tran et al. [18], Lopez et al. [20], Tangsathitkulchai et al. [22] and Seo et al. [47]). The char conversion, x, for the kinetic model is defined by,

$$x = \frac{(m_o - m_t)}{(m_o - m_f)} \tag{1}$$

where $m_o$is the initial mass in the gasification zone, m_t is the mass of char at time t, and m_f is the mass of ash. The derivative of the char conversion is calculated based on the central difference to maintain a second order accuracy:

$$\frac{dx}{dt} = \frac{x_{t+1} - x_{t-1}}{t_{t+1} - t_{t-1}} \tag{2}$$

Homogenous model was assumed as the carbon-gas reactions were uniformly distributed throughout the whole particle where the reactions occurred both outside and inside of the particle's surface [48, 49]. Therefore, the reaction rate for VM is defined as

$$\frac{dx}{dt} = k_{vm}(1 - x) \tag{3}$$

where k_{vm} is the kinetic rate constant of VM. The integral of equation (3) gives the following equation,

$$-\ln(x - 1) = k_{vm}t \tag{4}$$

Equation (4) finally gives the conversion from VM, x_{vm}, as

$$x_{vm} = 1 - \exp(-k_{vm}t) \tag{5}$$

The SCM assumes that the reactions gradually move inside from the external surface of char [49]. It is further considered that the reaction takes place on the surface of the grains assuming a spherical shape of the porous material [50]. The equation, as described by Levenspiel [51], is below:

$$\frac{dx}{dt} = k_{scm}(1 - x)^{\frac{2}{3}} \tag{6}$$

where k_{scm} is the rate constant of SCM. Integration of equation (6) gives the following solution,

$$3\left[1 - (1 - x)^{1/3}\right] = k_{scm}t \tag{7}$$

And, from equation (7), the value of x_{scm} can be determined as,

$$x_{scm} = 1 - \left(1 - \frac{k_{scm}t}{3}\right)^3 \tag{8}$$

The RPM was proposed by Bhatia and Perlmutter [52], which considers the physical structure change during the gasification reaction. The mathematical equation for RPM is:

$$\frac{dx}{dt} = k_{rpm}(1-x)\sqrt{(1-\psi\ln(1-x))} \tag{9}$$

where $k_{rpm}$is the rate constant of RPM and ψ is the structural parameter. The solution of equation (9) is derived as

$$\left({}^{2}/_{\psi}\right)\left[\sqrt{\left(1-\psi ln(1-x)\right)}-1\right] = k_{rpm}t \tag{10}$$

And, finally x_{rpm} is determined as

$$x_{rpm} = 1-\exp\left[-k_{rpm}t\left(1+\frac{k_{rpm}\Psi t}{4}\right)\right] \tag{11}$$

where the structural parameter, ψ, is defined as

$$\psi = \frac{4\pi L_o(1-\varepsilon_o)}{S_o^2} \tag{12}$$

In this equation, S_o is the initial surface area of char, ε_o is the total initial pore volume and L_o is the total initial pore length of char per unit volume. To find the value of ψ, some researchers proposed BET analysis [20-22, 53] through nitrogen adsorption isotherm, while some other researchers obtained the following equation (13) [54]. The value of ψ is determined by differentiating equation (9) as presented in the equation below.

$$\psi = \frac{2}{(2\ln(1-x_o)+1)} \tag{13}$$

where x_o is the conversion of char at the start of gasification.

A power law (PL) kinetic model is introduced based on the model presented in Tangsathikulchai et al. [22]. However, to form the new PL model developed in this research, the reaction time is non-dimensionalised first to fit with the char conversion, as below

$$x_{PL} = a\bar{t}^{b} \tag{14}$$

where x_{PL} is the PL conversion, a and b are the dimensionless values and $\bar{t}$ is the dimensionless value of time t/t_{max}. Through the values of a and b, the kinetic rate of the power law is determined as

$$k_{PL} = \frac{a^{1/b}\ b}{t_{max}} \tag{15}$$

The gasification rate, dx/dt, for the power law model is shown below,

$$\frac{dx}{dt} = k_{PL} x^{\left(1-\frac{1}{b}\right)} \tag{16}$$

The carbon reactivity of char for all the kinetic models is determined from the equation below [53, 55],

$$r_c = \frac{dx/dt}{1-x} \tag{17}$$

where r_c is the char reactivity, which depends on the conversion, temperature and gas composition [55]. Finally, the value of the activation energy is determined by the following equation.

$$k(T) = Ae^{-\frac{E_a}{R_u T}} \tag{18}$$

where A is the pre-exponential factor constant (min^{-1}), E_a is the activation energy (kJ/mol) and R_u is the gas constant (8.314 J $mol^{-1}K^{-1}$).

Kinetic results and discussion

As mentioned, this work aims at the investigation of the kinetic parameters of the FW char gasification based on the determination of the char conversion x, the gasification rate $\frac{dx}{dt}$, the reactivity r, the rate constant k, the activation energy E_a and the pre-exponential factor A in CO_2 environment. The result and discussion, therefore, includes the time dependent variation of x derived from each kinetic equation model; followed by the dependency of x on $\frac{dx}{dt}$ and r. Furthermore, the values of x and $\frac{dx}{dt}$ are compared among the VM, SCM, RPM and

PL, and the experiment results at different temperatures. Finally, the rate constant of the FW char in CO_2 gasification based on the best fitted kinetic model is presented.

Char conversion

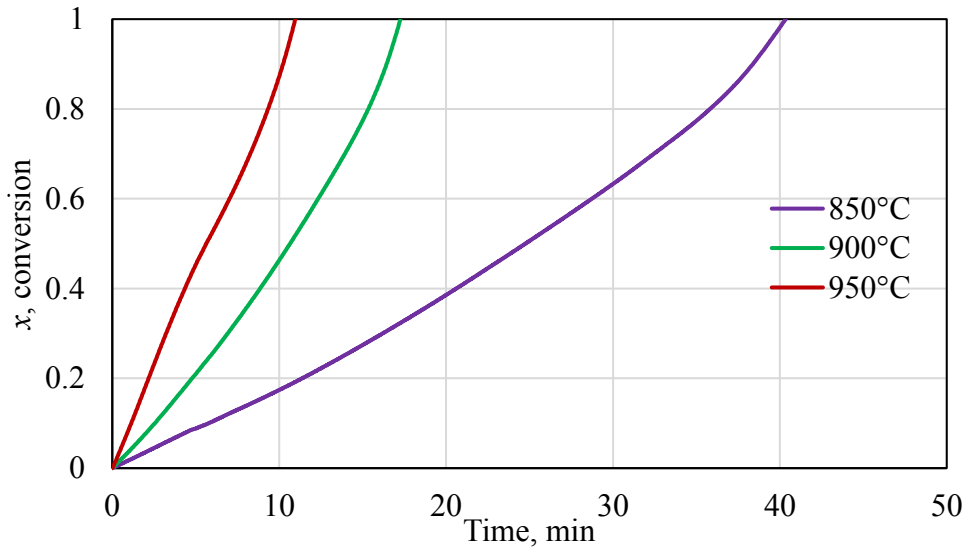

Figure 3 Mass conversion in the CO_2 gasification for the FW char at the temperatures of 850°C, 900°C and 950°C

The conversion of FW char is determined based on the CO_2 gasification process, as shown in Figure 3, and x is determined based on equation (1), from the beginning of CO_2 gasification until the process ended. Figure 3 presents the mass conversion for the FW char in the CO_2 gasification at 3 different temperatures, which shows that the char was converted rapidly at 950°C and it took approximately 11 minutes to be fully converted. At 900°C, it took 11 minutes to fully convert the char, while at 850°C, it took approximately 40 minutes. This therefore elucidates that the char was converted rapidly at a high temperature because the reactivity as well as collision of the char particles are enhanced at high temperature, and consequently sped up the char conversion [56]. This finding also agrees with the results reported in the literature but on different feedstock. For example, Lopez et al. [20] showed the conversion was quick in the CO_2 gasification of manure samples at high temperature. Kumar and Gupta [57] also presented that the high temperature has a rapid conversion for acacia and eucalyptus wood char in CO_2 gasification.

Gasification kinetic analyses

The kinetics application used to describe the experimental data obtained at 850°C, 900°C and 950°C for the FW char is shown in *Figure 4*, which represents the plots of $-\ln(x-1)$, $3\left[1-(1-x)^{1/3}\right]$, and $\left(2/\psi\right)\left[\sqrt{\left(1-\psi ln(1-x)\right)}-1\right]$ against time for VM, SCM and RPM, respectively. A linear line fit on each of the plots is then introduced to determine the corresponding reaction rate constant, k.

As seen in Figure 4 (a), k_{vm} for VM is determined respectively to be 0.0419 min^{-1}, 0.0971 min^{-1} and 0.1793 min^{-1} at 850°C, 900°C and 950°C with the corresponding R^2 of 63.5%, 64% and 70%. Therefore, the reaction rate constant is enhanced by the high temperature along with the increase of the value of R^2 suggesting better fitting. While for the SCM plot (Figure 4 (b)), the value of k_{scm} is 0.032 at 850°C indicating 81.7% R^2, at 900°C giving 0.0745 min^{-1} with 81.5% R^2, at 950°C giving 87.3% R^2 with 0.1345 min^{-1}. In addition, *Figure 4* (c) shows that k_{rpm} at 850°C was 0.0275 min^{-1} with R^2 81%, 0.0624 min^{-1} at 900°C with 82% R^2, then 0.1065 min^{-1} at 950°C with 88% R^2. The value of regression is thus increased further with the temperature rise for RPM.

Furthermore, of these three models, RPM is, thus far, the best fitted to the experimental data at R^2 81 - 88%, and the results presented also demonstrate that these kinetic models are sensitive to the experimental data obtained at various conditions, which is also clearly supported by the findings on the other various feedstocks already reported in the published literature. For example, Tomaszewich et al. [58] presented the VM, SCM and RPM models for coal chars CO_2 gasification, and showed that RPM gave better linearity graph. Whereas, Lopez et al. [20] found that SCM was the best fitted model for manure samples in CO_2 gasification, while Yuan et al. [21] presented M-RPM as the best fitted model with 99.6 – 99.7% R^2 in biomass char CO_2 gasification by using high temperature rapid pyrolysis. Kim et al. [49] studied CO_2 gasification of coal and showed that SCM was the best fitted in the biggest particle size, while VM was the best fitted for the smaller particle size.

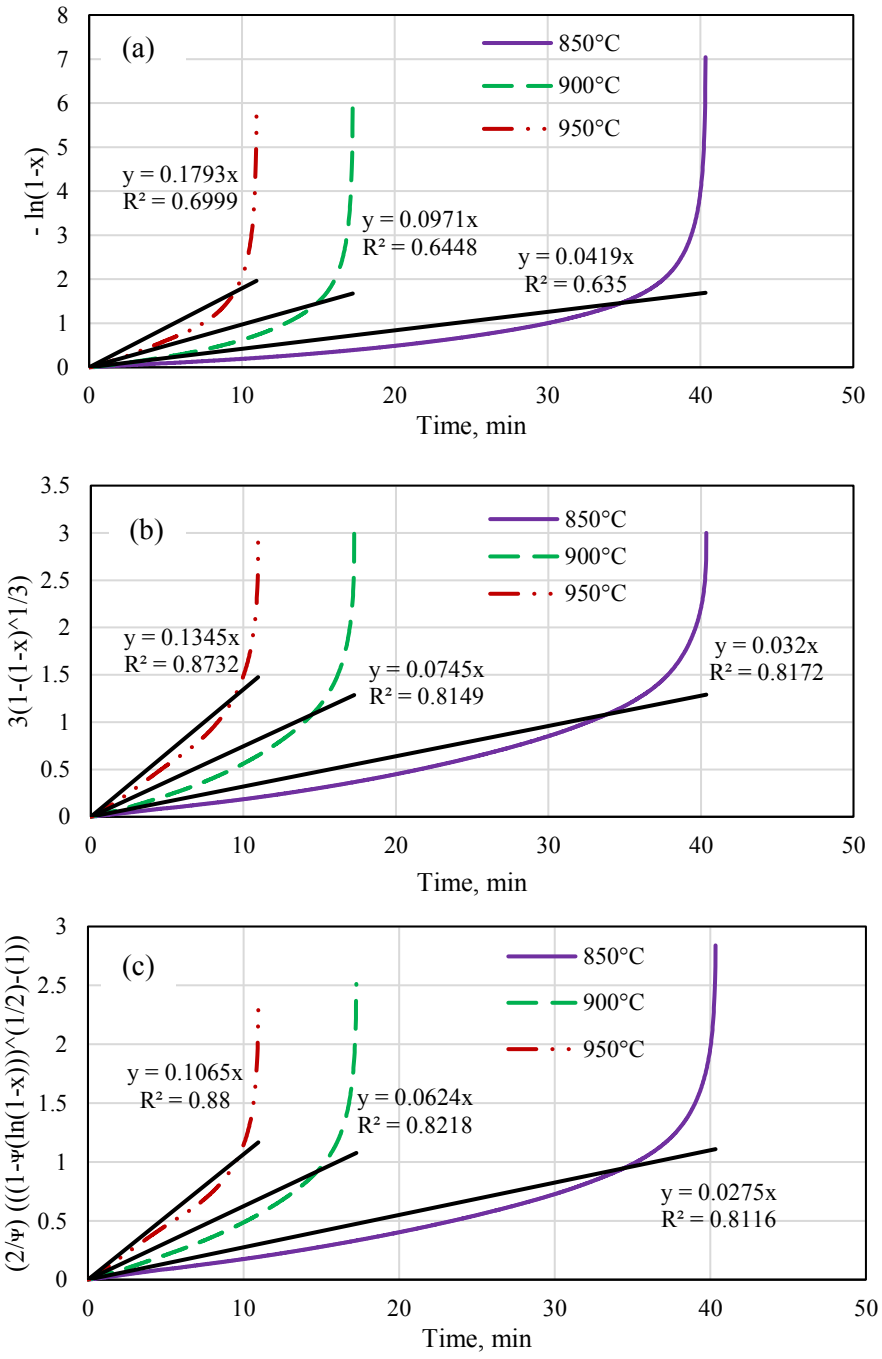

Figure 4 Application of the kinetic models for the FW char gasification at 850°C, 900°C and 950°C: (a) Volumetric model (VM), (b) Shrinking Core Model (SCM) and (c) Random Pore Model (RPM)

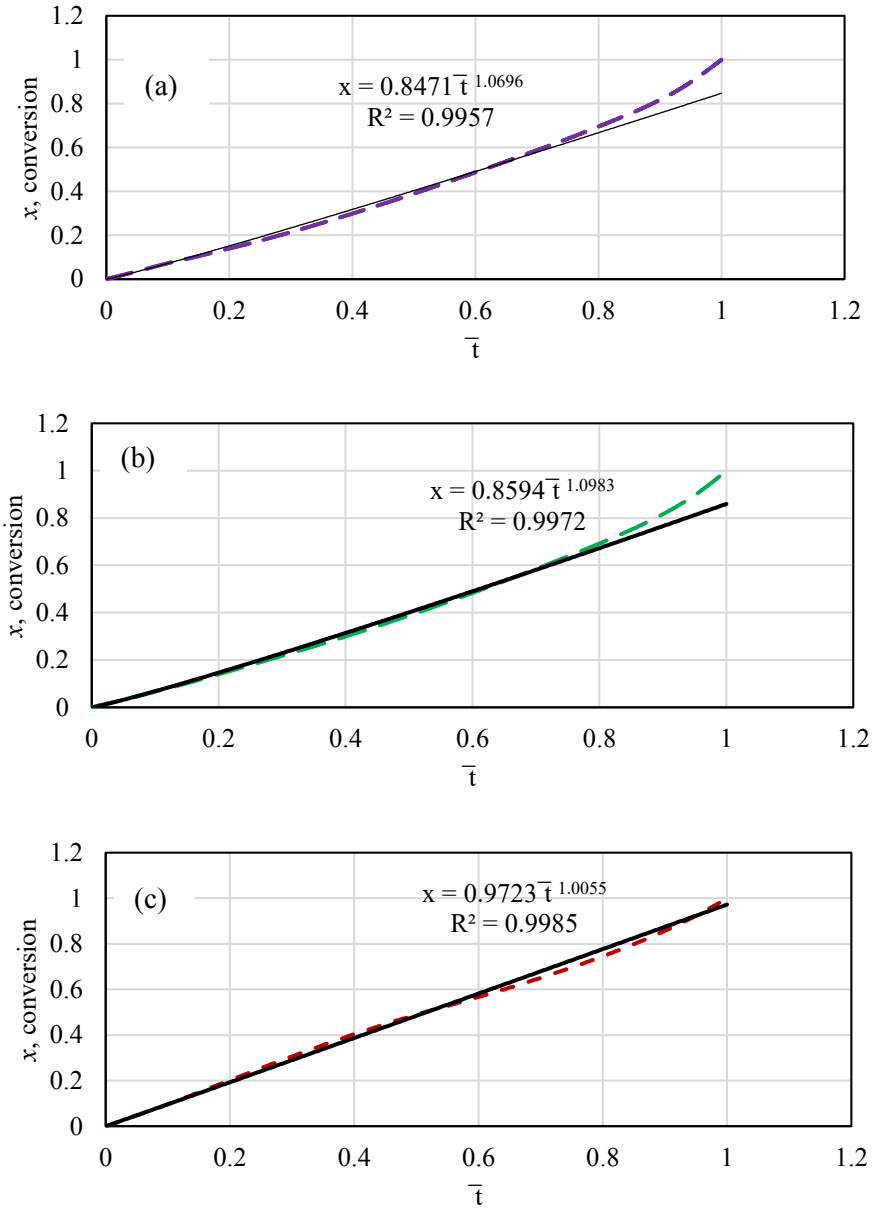

Figure 5 Power law model for FW char at the temperatures of (a) 850°C, (b) 900°C and (c) 950°C

In order to further improve the kinetic modelling for this research, the power-law, as described in equation (14), was introduced, and Figure 5 shows the conversion against $\bar{t}$ with the regression values. As shown in the graph, this model produced 99.6% R^2 at the temperature of 850°C, 99.7% R^2 at 900°C and 99.9% R^2 at 950°C, confirming an increase of the regression with the temperature increase. Based on the value of R^2 (> 99%), the power law seems to be the best fitted kinetic model for the experiment results.

Figure 6 compares the conversion of char over time obtained by all the kinetic models with the experimental results at different temperatures. The conversion of x_{vm} shows the biggest deviation from the experiment, followed by x_{scm}, x_{rpm} and then x_{PL}. Therefore, a ranking can be assigned as $x_{PL} > x_{rpm} > x_{scm} > x_{vm}$. In terms of the pattern, the conversions of VM, SCM and RPM are almost the same for every temperature, whereas PL produced the results best fitted with the experiment. Specifically, at the temperature of 850°C, the PL profile shows having the same result as from the experiment at the beginning. The predicted value becomes slightly higher from 7.7 minutes of the process until 23.4 minutes, then it is slightly lower from 28.9 minutes until at 40 minutes into the process. At 900°C, x_{PL} showed the same results with the experiment until 3 minutes of the process, then PL showed a small increase up to the experimental line. x_{PL} started to give the same result with the experimental data at around 13 minutes then it went slightly lower than the experimental data until the end. At the final temperature of 950°C, the value of x_{PL} is almost the same with experimental value from the beginning until 6.8 minutes, then the PL line started to increase, very slightly, until 10 minutes. Finally, it showed the same result with the experimental data until the end of the process. The kinetic parameters obtained from every model are summarized in Table 2 which also includes the corresponding regression values.

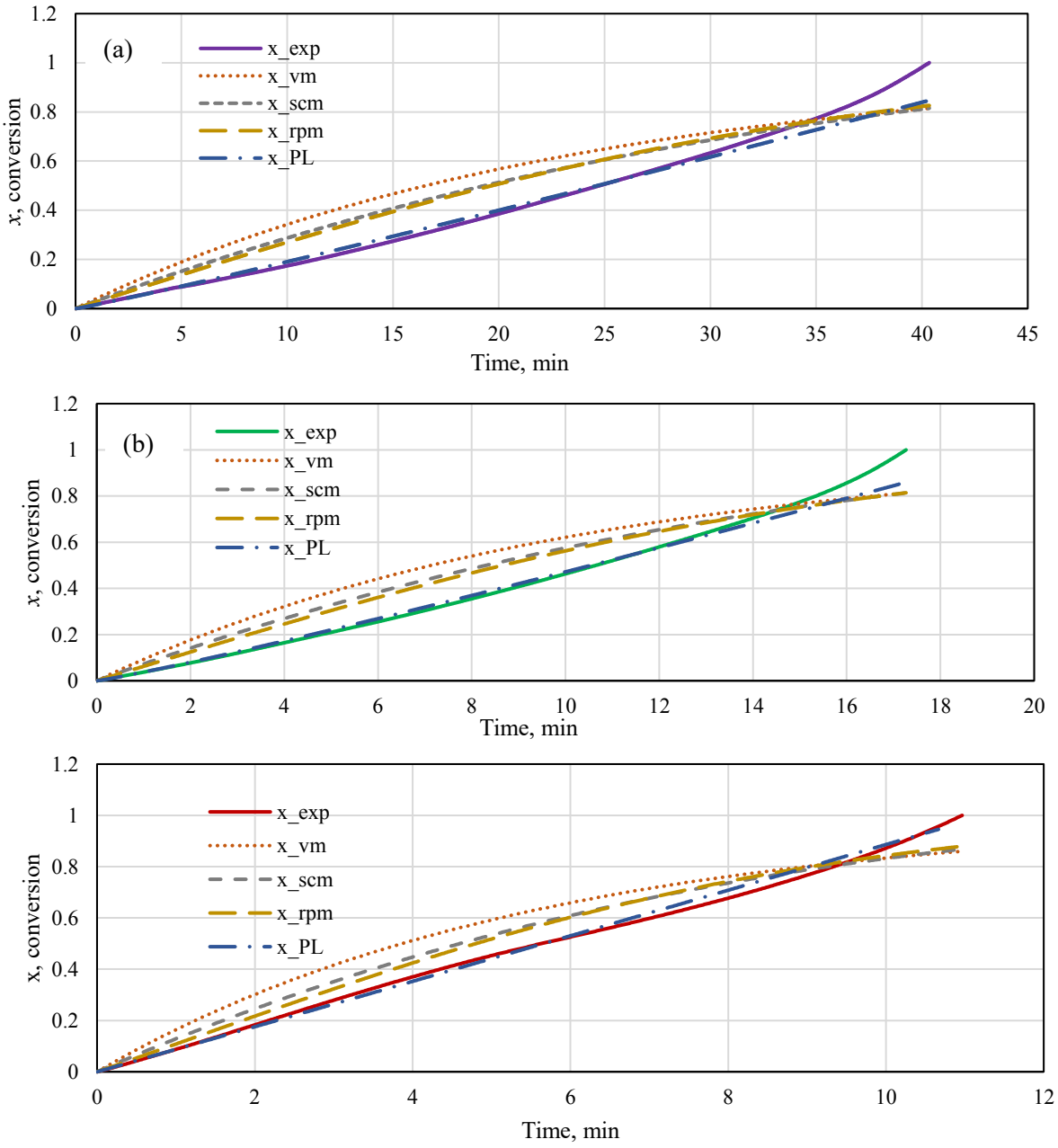

Figure 6 Comparison of conversion for the experimental, kinetic models and power-law fitting at the temperatures of (a) 850°C, (b) 900°C and (c) 950°C

Table 2 The kinetic models and parameters for FW char gasification at different temperatures

Temp (°C)	Model	Parameters				Regression, R^2(%)
		$k\ (min^{-1})$	ψ	a	b	
850	VM	0.0419				63.5
	SCM	0.032				81.72
	RPM	0.0275	2.08			81.16
	Power-law	0.0227		0.8471	1.0696	99.57
900	VM	0.0971				64.48
	SCM	0.0745				81.49
	RPM	0.0624	2.29			82.18
	Power-law	0.0554		0.8594	1.0983	99.72
950	VM	0.1793				69.99
	SCM	0.1345				87.32
	RPM	0.1065	2.78			88
	Power-law	0.0892		0.9723	1.0055	99.85

Table 2 presents the values of k for every model, ψ for RPM, and a and b for PL. It shows that the k values increased with the temperature for every model, because they were affected by the char conversion and time as already shown in Figure 4. For every temperature, the k values for VM were higher than those of others, followed by SCM, RPM and then PL. The values of k_{vm} and k_{scm} at 850°C are close to those for the CO_2 gasification of forest residues reported by Tran et al. [18] which are 0.043 min^{-1} and 0.030 min^{-1}. Furthermore, the value of ψ for FW char increased by raising the temperature, which was in the range of 2.08-2.78. Ahmed and Gupta [19] also showed the average value of ψ = 2.09 in the CO_2 gasification of woodchips, which is almost the same as the value found at the temperature of 850°C.

Gasification rate

The further validity of the kinetic models is also observed by comparing the gasification rates in experiments and the model predictions as shown in *Figure 7*.

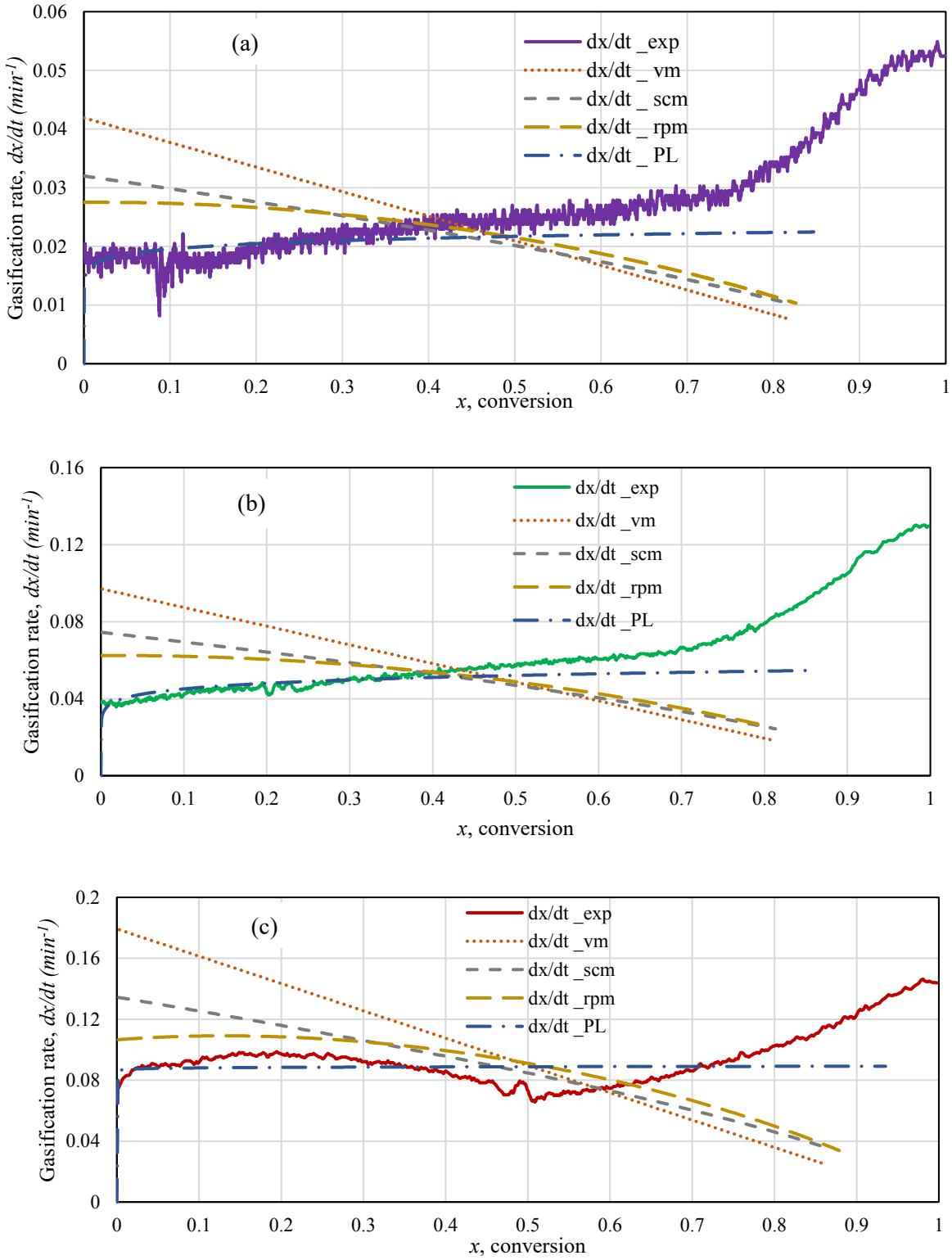

Figure 7 Gasification rate $\frac{dx}{dt}$ vs conversion for experimental, kinetic models and PL fitting at the temperatures of (a) 850°C, (b) 900°C and (c) 950°C

Figure 7 shows the gasification rate for experimental and other kinetic models at different temperatures where the conversion is considered until 0.8. At the temperature of 850°C, the gasification rate shows more fluctuation than the other results, because of a higher increase in conversion over time. The experimental data started to decrease at 0.08 conversion, then it increased until it crossed the PL line at 0.3 and continued to increase until 0.8 conversion. The gasification rate in the experimental data was not so different from the PL data. At 900°C, the gasification rate for the experimental data was lower than that of PL at the early stage, then it started to increase at 0.3 conversion until 0.8. At 950°C, the gasification rate for the experimental data was lower than PL until 0.02 conversion, then it increased until 0.2 conversion; later it decreased until conversion 0.5. Next, it increased until 1.0 conversion. As also shown in the figure that the difference between the experimental data and PL is not very different, which means PL is the best fitted to the experimental data in the gasification rate.

Further, based on the gasification rate equation, the rates for the other kinetic models, VM, SCM and RPM, decreased with the increase of conversion. Lopez et al. [50] mentioned that the rate for SCM decreased because of the surface area of each grain recedes during gasification as also demonstrated by Ollero et al. [55] for olive residue CO_2 gasification research. With regard to the effect of temperature, this clearly shows that the gasification rate is increased by raising the temperature. Based on the gasification rate, the reactivity r_c was determined as shown in equation (17), and the results are presented in the section below.

Char reactivity r_c

Figure 8 shows the comparison of the reactivity of FW char between the experimental and the kinetics model results including PL at different temperatures. As shown in this figure, the reactivity of char was lower at a low temperature, because the gasification rate, as presented in the section above, was higher at a high temperature. Based on the figure, it is shown that the value of the reactivity for VM was the same from the beginning until the end, because the reactivity of VM is equal to the value of rate constant k_{vm} according to the equations (3) and (17), while SCM and RPM showed increased reactivity with char conversion.

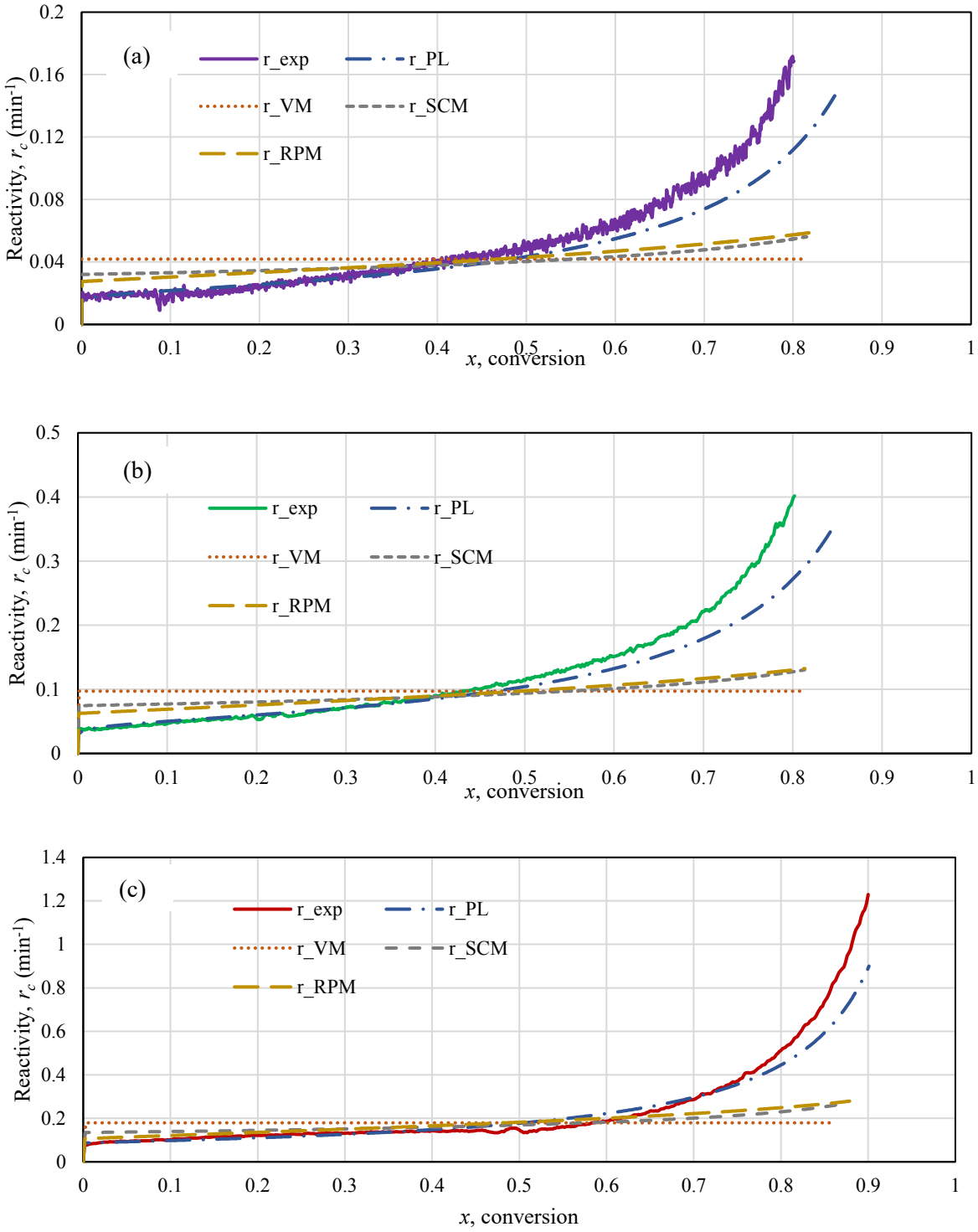

Figure 8 Comparison of the reactivity among experimental and kinetic models at the temperature of (a) 850°C, (b) 900°C and (c) 950°C

Further, Figure 8 (a) shows that the reactivity of char in the experimental result is slightly higher than the reactivity in PL. At the temperature of 900°C (Figure 8 (b)), the experimental result is smoother than at other temperatures. The experimental and PL have the

almost same results until the 0.4 conversion, and then the experimental data rises higher than the PL data until 0.8 conversion. At 950°C, Figure 8 (c) shows that the experimental results match with the PL results until 0.4 conversion, then it became slightly lower than the PL result. Finally, it increased until the end with an intersection at 0.7 conversion. Based on the result, it is further shown that PL demonstrates overall good agreement with the experimental result, while RPM showed the best result among the three other kinetic models. Additionally, it should be noted that the reactivity of char depends on the three characteristics of the samples; the chemical structures, the inorganic constituents and the porosity [38]. The reactivity was increased by increasing the char conversion because of the reaction of the inorganic components in the food waste which enhanced the catalytic effect. Moreover, the char contents in the food waste are high and they contain more salt [7]. The previous research by Kumar and Gupta [57] also showed the increase in reactivity with CO_2 gasification temperature for acacia and eucalyptus wood char, as to agree with this research.

Arrhenius plot

The values of the activation energy E_a and the pre-exponential factor A for every model are determined based on equation (18), and the results along with the other parameters for the linear equation for every kinetic model are presented in Table 3 and in Figure 9.

Table 3 : The linear equation, A and E_a for every kinetic model

Kinetics model	**Linear equation**	$\boldsymbol{A\ (min^{-1})}$	$\boldsymbol{E_a (kJmol^{-1})}$
VM	$y = -20\,004x + 14.664$	2 336 115	166.3
SCM	$y = -19\,763x + 14.185$	1 446 996	164.3
RPM	$y = -18\,645x + 13.043$	461 852	155.0
PL	$y = -18\,865x + 13.068$	473 544	156.8

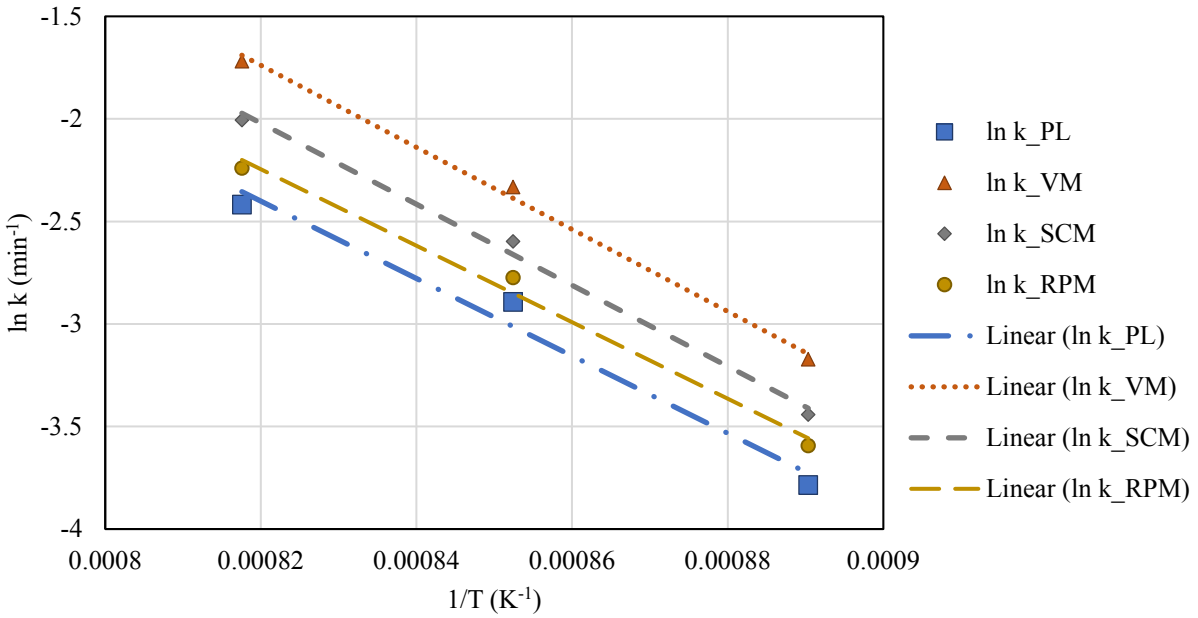

Figure 9 Arrhenius plot for FW char

Figure 9 shows the Arrhenius plots of the kinetic data determined for the FW char gasification at three different temperatures for every model. The PL presents the exponential factor A of 473 544 min^{-1} with the activation energy E_a of 156.8 kJ/mol. Among the three other kinetics models, RPM produced 461 852 min^{-1} of A and 155 kJ/mol of E_a, which are close to those of PL. Finally, the rate constant equation for the FW char in CO_2 gasification is expressed as $k_{PL} = 473\,544\, e^{\frac{-18865}{T}}$ based on PL, while it is expressed as $k_{RPM} = 461\,852\, e^{\frac{-18\,645}{T}}$ based on RPM. Furthermore, the Arrhenius plot shows no break in linearity as the temperature range is in the chemical reaction regime zone which also mentioned by Hungwe et al. [45], to show the significance of operation temperature range.

Conclusion

The kinetic study of FW char in isothermal CO_2 gasification was presented in this research based on VM, SCM, RPM and PL at the temperatures of 850°C, 900°C and 950°C. The char was pyrolyzed at the temperature of 800°C, and then sieved in the size range of 53 – 100µm before being analysed in the TGA. Based on the TGA-DTG profiles presented, the devolatilization zone as well as the CO_2 gasification zone was determined. From there, the conversion of char in CO_2 gasification was calculated to examine the kinetics by comparing the four aforementioned models. The value of k for each model is presented, which shows that the PL model is the best fitted based on the regression value. It shows higher than 99% regression, to obtain the value of A as 473 544 min^{-1} and E_a as 156.8 kJ/mol, which gave the

rate constant equation for the CO_2 gasification of FW char as $k_{PL} = 473\,544\, e^{\frac{-18865}{T}}$. RPM also gave the satisfied result even though the accuracy level is not as good as compared with PL, but the kinetic values obtained by these models were close. The rate constant equation for RPM was $k_{RPM} = 461\,852\, e^{\frac{-18645}{T}}$ with the activation energy of 155 kJ/mol. The kinetic parameters established through the models are currently being applied in investigating the CO_2 gasification of food waste in a gasifier for the production and optimisation of syngas.

Acknowledgement

The first author would like to acknowledge Majlis Amanah Rakyat (MARA) for funding her PhD research study at the University of Glasgow. She also acknowledges the University of Glasgow's mobility fund which supported her research visit to the Tokyo Institute Technology. The authors would also like to acknowledge Suzukakedai Materials Analysis Division, Technical Department, Tokyo Institute of Technology, for the ultimate and proximate analysis of the samples.

Nomenclature

A	Pre-exponential factor (min^{-1})
BET	Brunauer-Emmett-Teller
DEFRA	Department for Environment, Food and Rural Affairs
dx/dt	Gasification rate (min^{-1})
E_a	Activation energy
FW	Food waste
FWSC	Food waste supply chain
HM	Homogeneous model
k_{rpm}	Constant value of random pore model
k_{scm}	Constant value of Shrinking Core model
k_{vm}	Constant value of volumetric model
m_o	Initial mass in gasification zone
m_f	Mass of ash
m_t	Mass of char at time, t
MVRM	Modified volume-reaction model
PL	Power Law

R^2	Regression
r_c	Reactivity (min^{-1})
R_u	Universal gas constant (J/mol.K)
RPM	Random Pore Model
S_o	Initial surface area of char
SCM	Shrinking Core Model
t	Time
TGA	Thermogravimetric analyser
VM	Volumetric Model
x_o	Conversion of char at the start of gasification
x	Char conversion
x_{rpm}	Conversion of random pore model
x_{scm}	Conversion of Shrinking core model
x_{vm}	Conversion of volumetric model

Greek Symbol

ε_o	Total initial pore volume
L_o	Total initial pore length of char per unit volume
ψ	Structural parameter

References

1. DEFRA, *Digest of Waste and Resource Statistics - 2018 Edition* 2018, Department for Environment Food & Rural Affairs
2. Lin, C.S.K., Pfaltzgraff, L.A., Herrero-Davila, L., Mubofu, E.B., Abderrahim, S., Clark, J.H., Koutinas, A.A., Kopsahelis, N., Stamatelatou, K., Dickson, F., Thankappan, S., Mohamed, Z., Brocklesby, R. and Luque, R., *Food waste as a valuable resource for the production of chemicals, materials and fuels. Current situation and global perspective.* Energy & Environmental Science, 2013. **6**(2): p. 426-464.
3. Pfaltzgraff, L.A., De Bruyn, M., Cooper, E.C., Budarin, V. and Clark, J.H., *Food waste biomass: a resource for high-value chemicals.* Green Chemistry, 2013. **15**(2): p. 307-314.

4. Kiran, E.U., Trzcinski, A.P., Ng, W.J. and Liu, Y., *Bioconversion of food waste to energy: A review.* Fuel, 2014. **134**: p. 389-399.
5. Paritosh, K., Kushwaha, S.K., Yadav, M., Pareek, N., Chawade, A. and Vivekanand, V., *Food Waste to Energy: An Overview of Sustainable Approaches for Food Waste Management and Nutrient Recycling.* Biomed Research International, 2017.
6. Kataki, R., Chutia, R.S., Mishra, M., Bordoloi, N., Saikia, R. and Bhaskar, T., *Feedstock Suitability for Thermochemical Processes* in *Recent Advances in Thermochemical Conversion of Biomass* 2015, Elsevier
7. Ahmed, I.I. and Gupta, A.K., *Pyrolysis and gasification of food waste: Syngas characteristics and char gasification kinetics.* Applied Energy, 2010. **87**(1): p. 101-108.
8. Ko, M.K., Lee, W.Y., Kim, S.B., Lee, K.W. and Chun, H.S., *Gasification of food waste with steam in fluidized bed.* Korean Journal of Chemical Engineering, 2001. **18**(6): p. 961-964.
9. Tanaka, M., Ozaki, H., Ando, A., Kambara, S. and Moritomi, H., *Basic characteristics of food waste and food ash on steam gasification.* Industrial & Engineering Chemistry Research, 2008. **47**(7): p. 2414-2419.
10. Okajima, I., Shimoyama, D. and Sako, T., *Gasification and hydrogen production from food wastes using high pressure superheated steam in the presence of alkali catalyst.* Journal of Chemical Engineering of Japan, 2007. **40**(4): p. 356-364.
11. Marquez-Montesinos, F., Cordero, T., Rodriguez-Mirasol, J. and Rodriguez, J.J., *CO_2 and steam gasification of a grapefruit skin char.* Fuel, 2002. **81**(4): p. 423-429.
12. Bhat, A., Bheemarasetti, J.V.R. and Rao, T.R., *Kinetics of rice husk char gasification.* Energy Conversion and Management, 2001. **42**(18): p. 2061-2069.
13. Rapagna, S. and Latif, A., *Steam gasification of almond shells in a fluidised bed reactor: The influence of temperature and particle size on product yield and distribution.* Biomass & Bioenergy, 1997. **12**(4): p. 281-288.
14. Nanda, S., Isen, J., Dalai, A.K. and Kozinski, J.A., *Gasification of fruit wastes and agro-food residues in supercritical water.* Energy Conversion and Management, 2016. **110**: p. 296-306.
15. Ramzan, N., Ashraf, A., Naveed, S. and Malik, A., *Simulation of hybrid biomass gasification using Aspen plus: A comparative performance analysis for food, municipal solid and poultry waste.* Biomass & Bioenergy, 2011. **35**(9): p. 3962-3969.
16. Hla, S.S., Lopes, R. and Roberts, D., *The CO2 gasification reactivity of chars produced from Australian municipal solid waste.* Fuel, 2016. **185**: p. 847-854.
17. Tancredi, N., Cordero, T., RodriguezMirasol, J. and Rodriguez, J.J., *CO_2 gasification of eucalyptus wood chars.* Fuel, 1996. **75**(13): p. 1505-1508.
18. Tran, K.Q., Bui, H.H., Luengnaruemitchai, A., Wang, L. and Skreiberg, O., *Isothermal and non-isothermal kinetic study on CO_2 gasification of torrefied forest residues.* Biomass & Bioenergy, 2016. **91**: p. 175-185.
19. Ahmed, I.I. and Gupta, A.K., *Kinetics of woodchips char gasification with steam and carbon dioxide.* Applied Energy, 2011. **88**(5): p. 1613-1619.
20. Fernandez-Lopez, M., Lopez-Gonzalez, D., Valverde, J.L. and Sanchez-Silva, L., *Kinetic study of the CO_2 gasification of manure samples.* Journal of Thermal Analysis and Calorimetry, 2017. **127**(3): p. 2499-2509.
21. Yuan, S., Chen, X.L., Li, J. and Wang, F.C., *CO_2 gasification kinetics of biomass char derived from high-temperature rapid pyrolysis.* Energy and Fuels, 2011. **25**(5): p. 2314-2321.
22. Tangsathitkulchai, C., Junpirom, S. and Katesa, J., *Comparison of Kinetic Models for CO_2 Gasification of Coconut-Shell Chars : Carbonization Temperature Effects on*

Char Reactivity and Porous Properties of Produced Activated Carbons Engineering Journal 2013. **17**(1).
23. Rollinson, A.N. and Karmakar, M.K., *On the reactivity of various biomass species with CO2 using a standardised methodology for fixed-bed gasification.* Chemical Engineering Science, 2015. **128**: p. 82-91.
24. Gomez, A. and Mahinpey, N., *Kinetic study of coal steam and CO2 gasification: A new method to reduce interparticle diffusion.* Fuel, 2015. **148**: p. 160-167.
25. Parvez, A.M., Mujtaba, I.M., Pang, C.H., Lester, E. and Wu, T., *Effect of the addition of different waste carbonaceous materials on coal gasification in CO2 atmosphere.* Fuel Processing Technology, 2016. **149**: p. 231-238.
26. Prabowo, B., Aziz, M., Umeki, K., Susanto, H., Yan, M. and Yoshikawa, K., *CO_2-recycling biomass gasification system for highly efficient and carbon-negative power generation.* Applied Energy, 2015. **158**: p. 97-106.
27. Kumar, U. and Paul, M.C., *CFD modelling of biomass gasification with a volatile break-up approach.* Chemical Engineering Science, 2019. **195**: p. 413-422.
28. Salem, A.M., Kumar, U., Izaharuddin, A.N., Dhami, H., Sutardi, T. and Paul, M.C., *Advanced Numerical Methods for the Assessment of Integrated Gasification and CHP Generation Technologies.* Coal and Biomass Gasification: Recent Advances and Future Challenges, 2018: p. 307-330.
29. Sepe, A.M., Li, J. and Paul, M.C., *Assessing biomass steam gasification technologies using a multi-purpose model.* Energy Conversion and Management, 2016. **129**: p. 216-226.
30. Sutardi, T., Paul, M.C. and Karimi, N., *Investigation of coal particle gasification processes with application leading to underground coal gasification.* Fuel, 2019. **237**: p. 1186-1202.
31. Silaen, A. and Wang, T. *Comparison of instantaneous, equilibrium, and finite-rate gasification models in an entrained-flow coal gasifier*. in *Proceedings of the 26th International Pittsburgh Coal Conference*. 2009. Citeseer.
32. Silaen, A. and Wang, T., *Effect of turbulence and devolatilization models on coal gasification simulation in an entrained-flow gasifier.* International Journal of Heat and Mass Transfer, 2010. **53**(9-10): p. 2074-2091.
33. Alganash, B., Paul, M.C. and Watson, I.A., *Numerical investigation of the heterogeneous combustion processes of solid fuels.* Fuel, 2015. **141**: p. 236-249.
34. Chen, C.-J., Hung, C.-I. and Chen, W.-H., *Numerical investigation on performance of coal gasification under various injection patterns in an entrained flow gasifier.* Applied energy, 2012. **100**: p. 218-228.
35. Li, Z., Wei, F. and Jin, Y., *Numerical simulation of pulverized coal combustion and NO formation.* Chemical engineering science, 2003. **58**(23-24): p. 5161-5171.
36. Watanabe, H. and Otaka, M., *Numerical simulation of coal gasification in entrained flow coal gasifier.* Fuel, 2006. **85**(12-13): p. 1935-1943.
37. Boiko, E. and Pachkovskii, S., *A kinetic model of thermochemical transformation of solid organic fuels.* Russian journal of applied chemistry, 2004. **77**(9): p. 1547-1555.
38. Di Blasi, C., *Combustion and gasification rates of lignocellulosic chars*. 2009. p. 121-140.
39. Molina, A. and Mondragón, F., *Reactivity of coal gasification with steam and CO_2.* 1998. p. 1831-1839.
40. Jayasena, D.D., Ahn, D.U., Nam, K.C. and Jo, C., *Flavour Chemistry of Chicken Meat: A Review.* Asian-Australasian Journal of Animal Sciences, 2013. **26**(5): p. 732-742.

41. Mottram, D.S., *Flavour formation in meat and meat products: a review.* Food Chemistry, 1998. **62**(4): p. 415-424.
42. Tang, J., Jin, Q.Z., Shen, G.H., Ho, C.T. and Chang, S.S., *Isolation and Identification of Volatile Compounds from Fried Chicken.* Journal of Agricultural and Food Chemistry, 1983. **31**(6): p. 1287-1292.
43. Butnariu, M. and Butu, A., *Chemical composition of Vegetables and their products.* Handbook of Food Chemistry, 2015: p. 627-692.
44. Kim, D., Yoshikawa, K., Lee, K. and Park, K.Y., *Investigation of the combustion characteristics of municipal solid wastes and their hydrothermally treated products via thermogravimetric analysis.* Journal of Material Cycles and Waste Management, 2015. **17**(2): p. 258-265.
45. Hungwe, D., Ding, L., Khoshbouy, R., Yoshikawa, K. and Takahashi, F., *Kinetics and Physicochemical Morphology Evolution of Low and High-Ash Pyrolytic Tire Char during CO2 Gasification.* Energy & Fuels, 2020. **34**(1): p. 118-129.
46. Trivedi, M.K., Dixit, N., Panda, P., Sethi, K.K. and Jana, S., *In-depth investigation on physicochemical and thermal properties of magnesium (II) gluconate using spectroscopic and thermoanalytical techniques.* Journal of Pharmaceutical Analysis, 2017. **7**(5): p. 332-337.
47. Seo, D.K., Lee, S.K., Kang, M.W., Hwang, J. and Yu, T.U., *Gasification reactivity of biomass chars with CO_2.* Biomass & Bioenergy, 2010. **34**(12): p. 1946-1953.
48. Ye, D.P., Agnew, J.B. and Zhang, D.K., *Gasification of a South Australian low-rank coal with carbon dioxide and steam: kinetics and reactivity studies.* Fuel, 1998. **77**(11): p. 1209-1219.
49. Kim, Y.T., Seo, D.K. and Hwang, J., *Study of the Effect of Coal Type and Particle Size on Char-CO_2 Gasification via Gas Analysis.* Energy & Fuels, 2011. **25**(11): p. 5044-5054.
50. Lopez-Gonzalez, D., Fernandez-Lopez, M., Valverde, J.L. and Sanchez-Silva, L., *Gasification of lignocellulosic biomass char obtained from pyrolysis: Kinetic and evolved gas analyses.* Energy, 2014. **71**: p. 456-467.
51. Levenspiel, O., *Chemical Reaction Engineering* Third Edition ed. 1999.
52. Bhatia, S.K. and Perlmutter, D.D., *A Random Pore Model for Fluid-Solid Reactions .1. Isothermal, Kinetic Control.* Aiche Journal, 1980. **26**(3): p. 379-386.
53. Alvarez, J., Lopez, G., Amutio, M., Bilbao, J. and Olazar, M., *Kinetic Study of Carbon Dioxide Gasification of Rice Husk Fast Pyrolysis Char.* Energy & Fuels, 2015. **29**(5): p. 3198-3207.
54. Ochoa, J., Cassanello, M.C., Bonelli, P.R. and Cukierman, A.L., *CO_2 gasification of Argentinean coal chars: a kinetic characterization.* Fuel Processing Technology, 2001. **74**(3): p. 161-176.
55. Ollero, P., Serrera, A., Arjona, R. and Alcantarilla, S., *The CO_2 gasification kinetics of olive residue.* Biomass & Bioenergy, 2003. **24**(2): p. 151-161.
56. Logan, S.R., *Fundamentals of Chemical Kinetics* 1996: Harlow: Longman, 1996.
57. Kumar, M. and Gupta, R.C., *Influence of Carbonization Conditions on the Gasification of Acacia and Eucalyptus Wood Chars by Carbon-Dioxide.* Fuel, 1994. **73**(12): p. 1922-1925.
58. Tomaszewicz, M., Labojko, G., Tomaszewicz, G. and Kotyczka-Moranska, M., *The kinetics of CO_2 gasification of coal chars.* Journal of Thermal Analysis and Calorimetry, 2013. **113**(3): p. 1327-1335.